Available online at www.eccomasproceedia.org
Eccomas Proceedia SMART (2023) 355-366

ECCOMAS
Proceedia

X ECCOMAS Thematic Conference on Smart Structures and Materials
SMART 2023
D.A. Saravanos, A. Benjeddou, N. Chrysochoidis and T. Theodosiou (Eds)

SMA BASED ADAPTIVE STRUCTURE DEMONSTRATOR FOR AN OVERLAND LOW BOOM SUPERSONIC VEHICLE

JAMES MABE, DARREN HARTL, DIMITRIS C. LAGOUDAS, BENJAMIN MCADAMS, AND RYAN TROUT

Aerospace Engineering and Materials Science and Engineering
Texas A&M University, College Station, TX 77843. USA
Email: jim.mabe@tamu.edu

Abstract.

In this paper a series of low boom adaptive structure hardware demonstrators are described. The designs are enabled by recent advances in SMA technology including improved high temperature materials, better design and modeling tools, and industry approved test methods. The test hardware replicates the centerline keel of a representative supersonic aircraft. An array of SMA based actuators are used to modify the keel structure resulting in a change to the geometry of the Outer Mold Line (OML). The shape changes are intended to maintain a low boom signature in response to changes in Mach, angle of attack, flight path, or atmospheric profile. A description of the hardware design, SMA control system, and integration into a supersonic flight simulator are shown. Test results showing real-time geometry changes minimizing the predicted boom are presented. The design, build, and test of the adaptive structure demonstrators was led by a team of undergraduate students, supported by university faculty and industry advisors. The results presented are outcomes of Texas A&M University's Adaptive Aerostructures for Revolutionary Civil Supersonic Transportation project sponsored by NASA's University Leadership Initiative (ULI).

Keywords: Smart Structures, Supersonic, Adaptive Structures, Shape Memory Alloys, Sonic Boom, Actuators, Low Boom.

1 INTRODUCTION

To enable the return to flight of civil supersonic aircraft, vehicle designs must move beyond traditional aerodynamic performance metrics to include the shaping of sonic boom signatures to minimize perceived loudness across a wide range of conditions. A vehicle's Mach, angle of attack, and atmospheric profile between the aircraft and the ground have all been shown to have a significant impact on perceived loudness. However, studies have shown that during these adverse boom circumstances small modifications to the geometry of the vehicle's outer mold line (OML) can restore the vehicle to a low boom state [1-5]. In addition to low boom, numerous other applications have been identified where adaptive structures could enable optimized aircraft performance across all operating scenarios, some of these are shown in **Fig. 1**.

A multidisciplinary team led by Texas A&M University is investigating commercially viable

Peer-review under responsibility of the organizing committee of SMART 2023.
doi: 10.7712/150123.9791.444611

civil supersonic transport aircraft that can modify their shape during flight under a range of conditions to meet noise and efficiency requirements for overland flight. This project is sponsored under NASA's University Leadership Initiative (ULI) program. To be commercially viable, a supersonic transport must be able meet low boom noise limits for all flight conditions. This require aircraft to be able to adapt and reconfigure to changing flight conditions to maintain a low boom signature.

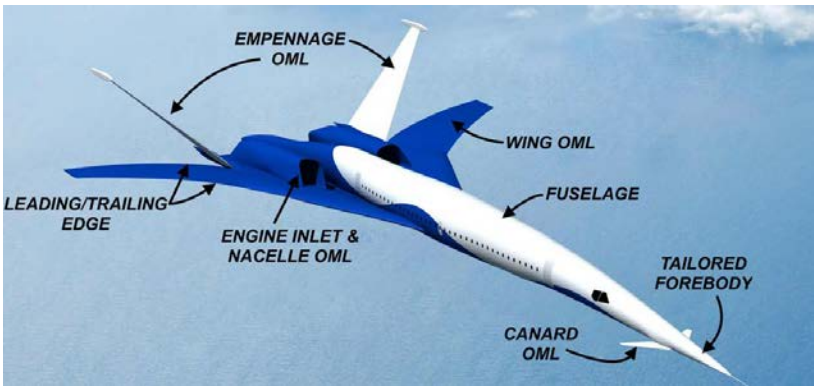

Figure 1: Adaptive Structures Applications

To support the optimization of OML shapes changes that mitigate perceived noise at off-design conditions a tool chain was developed that utilized reduced order and high-fidelity computational fluid dynamics (CFD) for near field evaluation of the pressures and shocks, tools to estimate propagation of the shocks through the atmosphere below the vehicle, and tools to translate the ground pressure signal to perceived noise [2]. This tool chain is shown in **Fig 2**.

Shape memory alloy (SMA) based actuators were selected for this application as they can provide a compact and light weight distributed system that enables real-time shape changes to the outer mold line (OML) of the aircraft. Geometric reconfiguration impacts the boom signature and maintains optimal low-boom and low-drag configurations across all environments and flight conditions [6].

NiTiHf High Temperature SMAs (HTSMAs) were selected as the baseline material. HTSMAs prevent inadvertent actuation, as the martensite finish temperature is below any anticipated operational ambient temperatures for aircraft parts, specified as 85°C. It is also important to minimize the Austenite finish temperature to limit the power needed for full actuation. Additionally, a 100,000 cycle lifetime at actuation strains greater than 2% was specified to support practical

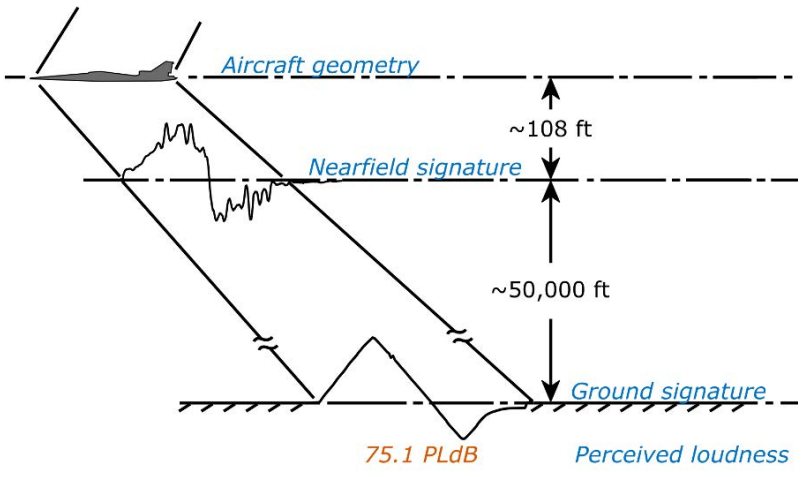

Figure 2: Tool Chain for Analysis and Optimization of Aircraft Geometries for Low Boom

commercial applications..

In **Fig. 3** the primary parameters driving durability and operational lifecycles are shown of SMA actuators are shown, including composition, processing, and operations.

To realize the maximum benefits of adaptive structures design, integration, and operation of adaptive structures must be feasible and cost effective. This adaptive structures material development, modeling, and design process is shown in **Fig. 4**..

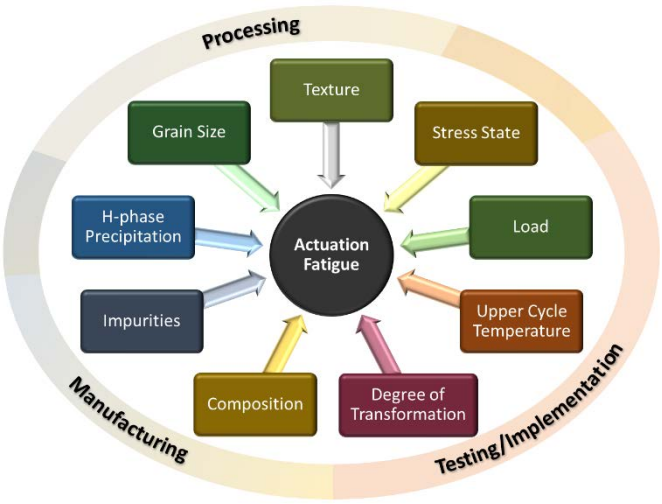

Figure 3: Shape Memory Alloy Development

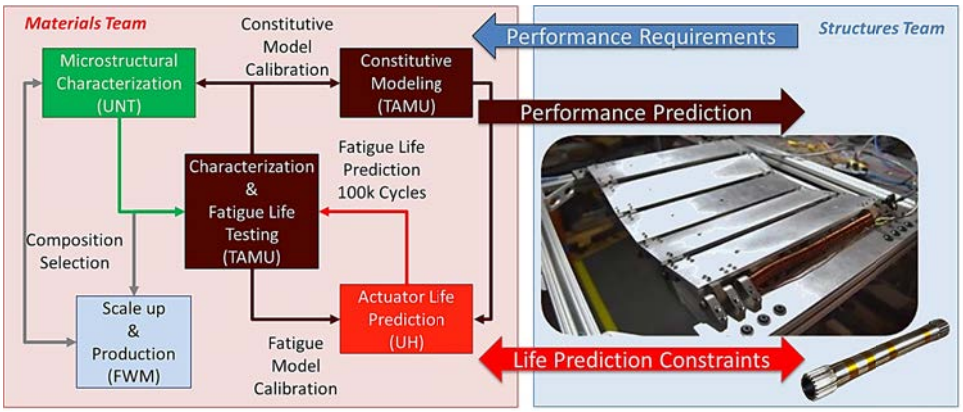

Figure 4: Shape Memory Alloy System Level Development and Modeling

3 HARDWARE DEMONSTRATORS

To fully validate the adaptive structures design tools and demonstrate performance a series of hardware demonstrators were designed, built, and tested. Each design represented the keel surface of NASA's X-59 low boom demonstrator. Each adaptive structure demonstrator had an increased level of complexity and shape control capability.

3.1 1D Segmented panel demonstrator.

The first demonstration of an adaptive geometry for low boom supersonic vehicles is shown in **Fig. 5** utilizing a single linear SMA based actuator acting on a panel composed of an elastomer sheet with rigid aluminum panels bonded on the outer surface to control shape and provide impact resistance. The linear actuator uses an SMA torsional tube component made

from nearly equiatomic NiTi. A rack and pinion assembly converts the SMA's rotary motion to linear displacement. A micro induction heating system was used to heat the SMA tube and small fans (not shown) cooled the tube. A spring was attached to the linear output of the rack and pinion assembly to provide a restoring force that supplemented the 2-way shape memory effect that was trained into the SMA tube. The sensor and control system was based on a small, locally mounted, Linux based computer that monitored temperatures using type-K thermocouples, SMA tube rotation using a digital encoder, and Pulse Width Modulation (PWM) outputs to control induction power and SMA heating. The measured tube rotation was used for feedback control and to determine linear motion on the panel surface. The entire control system is compact with the sensors, actuator, and control system co-located near the adaptive surface. Power and a communications link to command setpoints and received data are the only external components. Full closed loop control of the surface's mid-point height and subsequent shape

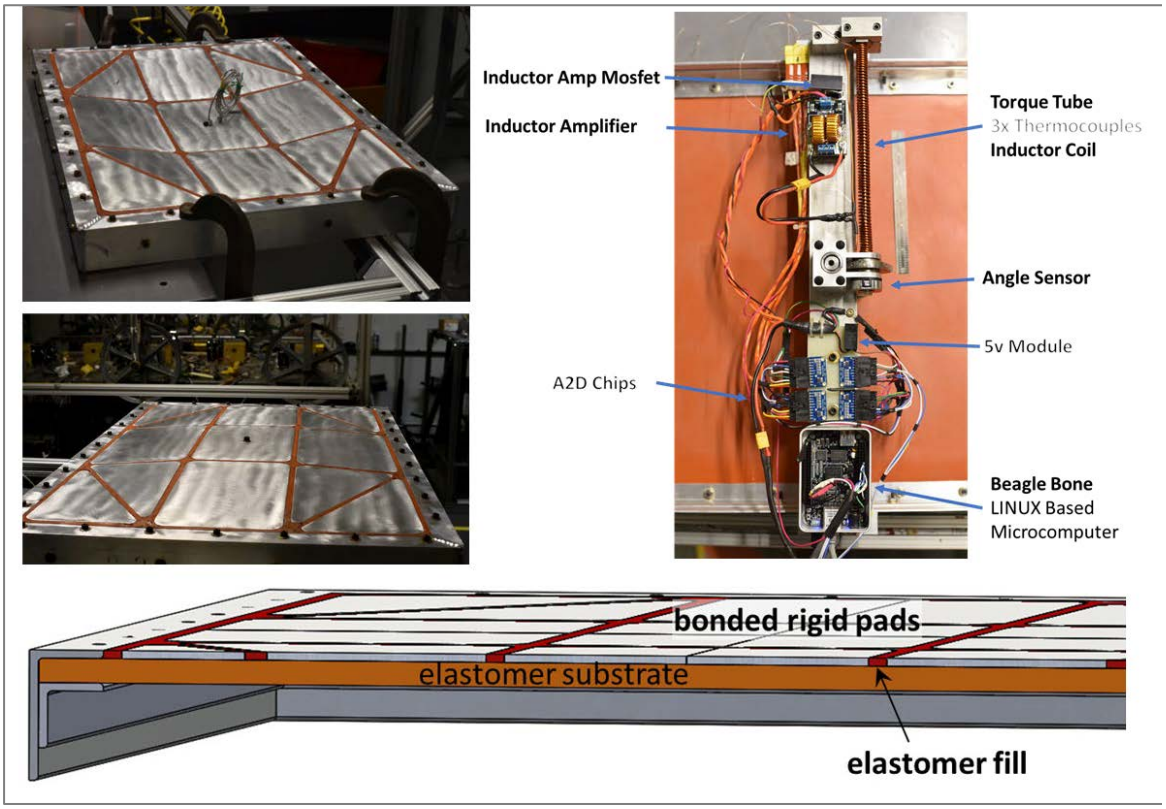

Figure 5: Segmented Panel Morphing Surface

was is shown in **Fig. 6**. Induction heating enables rapid response to changes in the position setpoint and minimizes overshoot. As with many SMA applications, cooling is the rate limiting process. However, previous work has demonstrated accelerated cooling methods such as compressed air routed down the inner diameter of the tube.

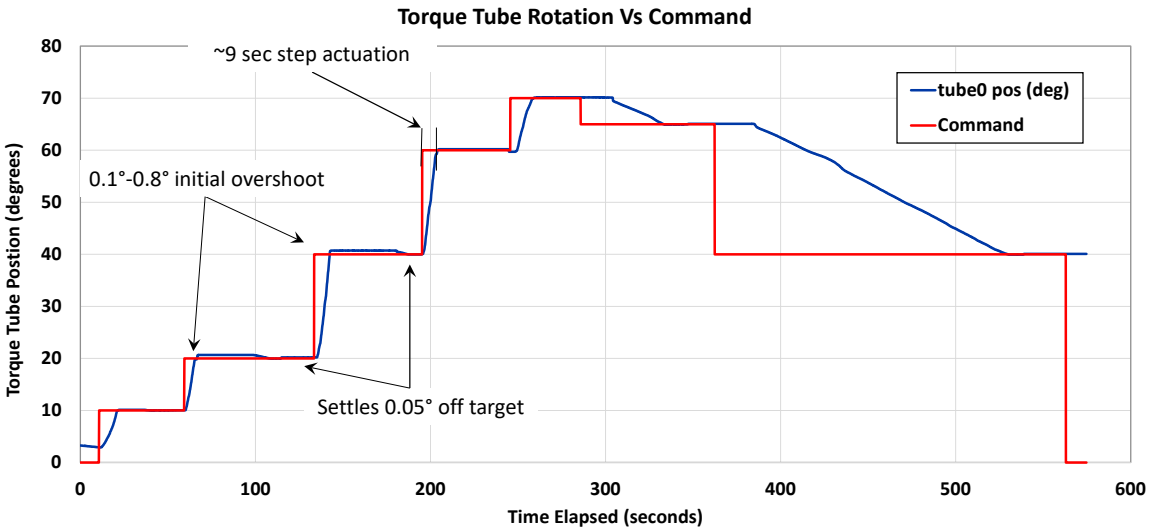

Figure 6: Closed Loop Control of Segmented Panel

3.2 Five panel adaptive surface

Building on the success of the first 1D proof of concept demonstration, a second variable geometry surface was designed, built, and tested. The design and assembly are shown in **Fig. 7**. The elastomer base was replaced by panels connected with rigid hinges to reduce weight and eliminate excessive compliance. Multiple actuators were added to increase the range of

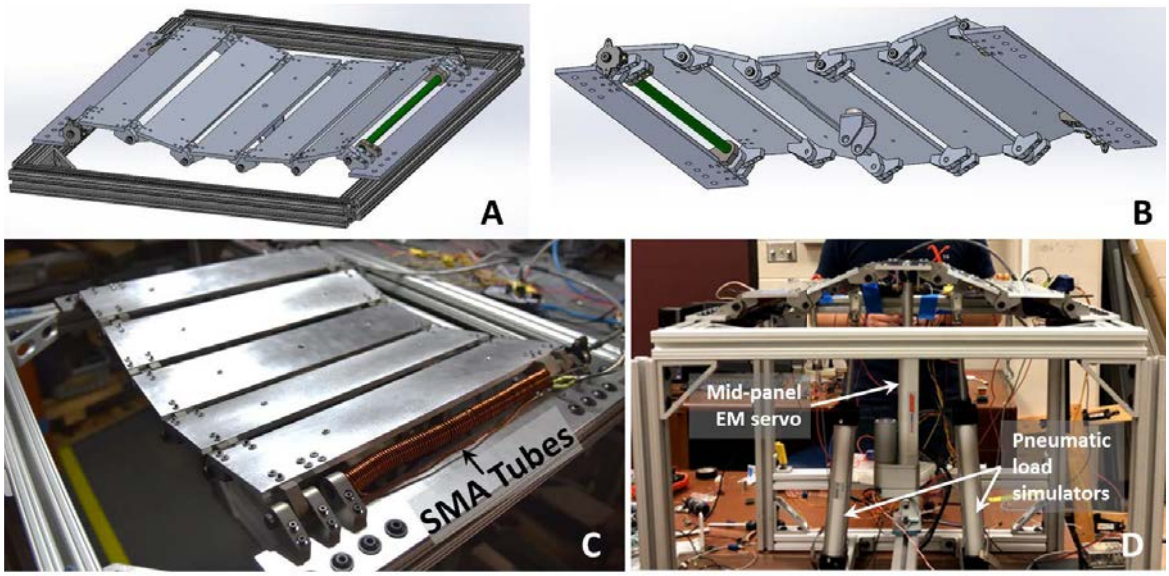

Figure 7: 1x5 Panel Adaptive Surface. Two SMA Torsion Actuators and One Linear Servo. Pneumatic Actuators to Provide Simulated Aerodynamic Loads

controllable shapes. Two SMA torsional actuators were integrated into the hinge of the edge panels to control angle of the panel, while the mid-panel's height was controlled with a linear electric servo. The SMA torsional actuator was attached and fixed at one end to the exterior fixed structure and the other end was attached to the end panel. When the trained tube is heated the SME causes the tube to shear along its length resulting in a rotation at the panel end which deflects the panel to the desired angle. Both tubes had been trained in 2-way SME and no restoring forces were used to return the panel to its base position. Two pneumatic actuators were integrated into the test bed to provide forces that simulate the surface loads the panel would see in flight.

A control system similar to what was used in the 1D panel was integrated into the system. SMA temperatures, panel angles, and the mid-panel height were measured by the Linux based micro computer using custom python code. Shape commands were communicated to the system from a remote PC, while additional Python control code managed heater power, compressed air cooling, and linear servo position. Motion between each of the actuators was coordinated to account for the unique kinematics of the panel as seen in **Fig. 8**. The test bed represents a section

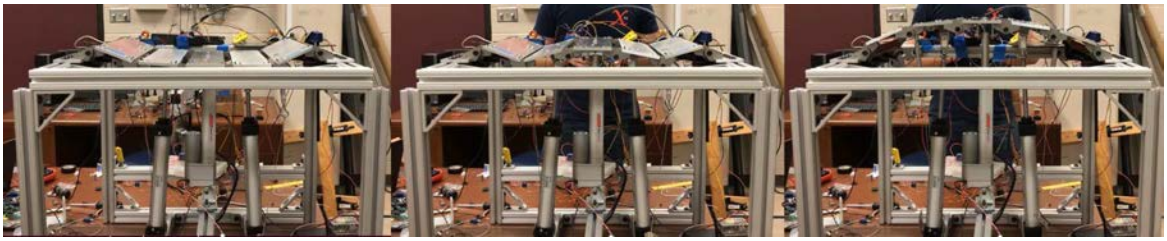

Figure 8: 1x5 Panel Range of Actuation

of the keel line of a supersonic vehicle and is oriented in the inverted position for testing purposes. The rigid hinges connecting the panels create a fixed length for the 5 panels from edge hinge to edge hinge. In the left and right pictures shown in **Fig. 8** the arc of the negative surface and positive surfaces is a smooth arch equal to the total length of the panels and hinges. However, to pass the surface through the midpoint the total length of the panels exceeds the flat distance between outer hinges and the panels must be folded to shorten overall length. This feature significantly limited the available shapes that could be generated, including asymmetrical shapes.

Testing was performed over a range of conditions including constant simulated surface loads and surface loads that varied as a function of shape. The varying surface loads represented expected pressures on the center keel line of a supersonic jet. These loads varied from positive to negative depending on whether the panel deformation was a dent or a bump. In a dent shape (left picture in **Fig. 8**) the surface loads are negative and tend to pull the surface out away from the vehicle and assist the SMA actuation. When the surface is a bump (right picture in **Fig. 8**) the surface loads are positive and tend to push the surface towards the vehicle center and resist the SMA actuation.

Test data of a complete translation of the 5 panel surface from dent to bump with constant surface loads is shown in **Figure 9**. In graphs A and B the edge panel angles are shown following the setpoints with minimal overshoot or oscillations. Control was similar for both negative and positive surface loads. In graphs C and D the temperature of the SMA is shown. In graph C the surface loads were positive and worked against the SMA actuation resulting in higher SMA temperatures than are shown in graph D, where the surface loads are negative and assist the SMA actuation.

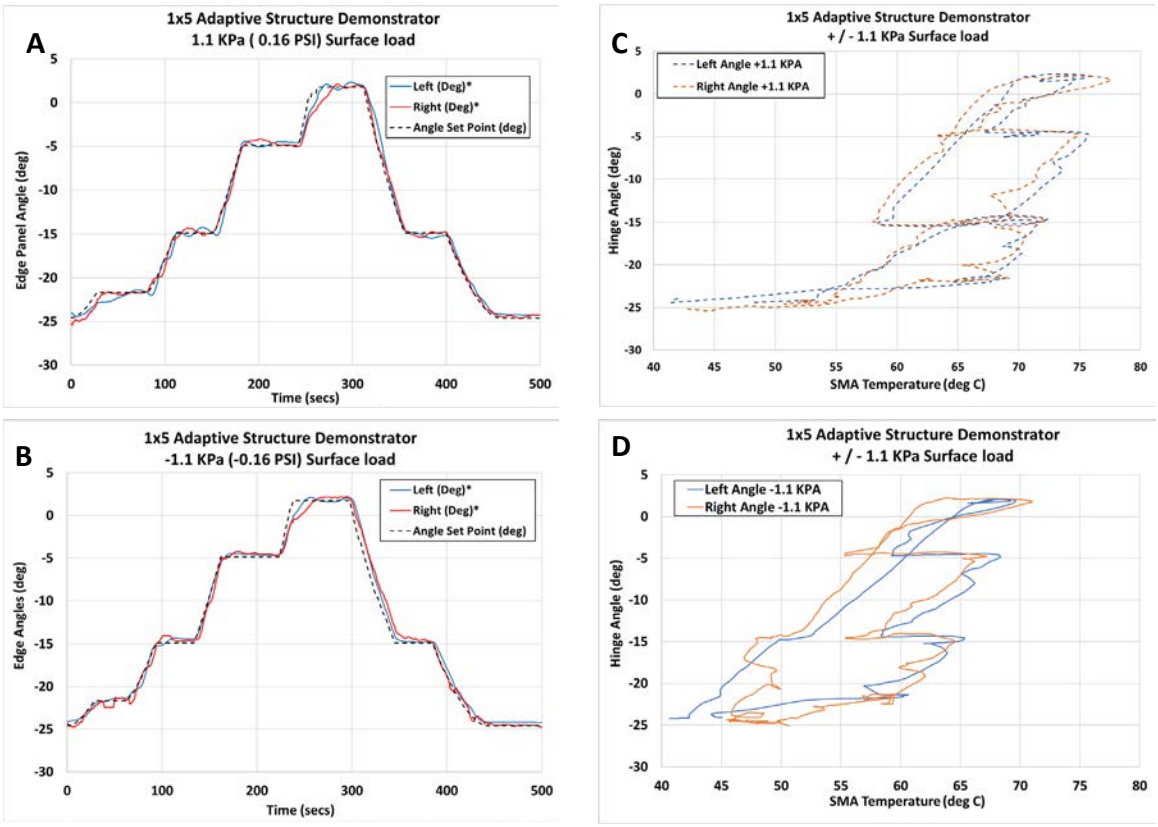

Figure 9: 1x5 panel shape control with simulated aerodynamic loading.

Results for testing of the five panel surface's ability to hold shape while surface loads changed are shown in **Figure 10**. This represents the effect of a sudden change in Mach or angle of attack that would cause a sudden change in loads. The upper graph in **Figure 10** shows the panel height at -25mm (a dent) and +25mm (a bump). While holding that surface shape the pneumatic system was used to quickly sweep between maximum and minimum loading.

In the lower graph the edge panel angles are shown to fluctuate somewhat, but generally hold position. The SMA temperatures are shown to vary more than 30 degrees as the surface loads go from assisting the SMA forces to reacting against the SMA. This is especially evident between approximately 500 and 800 seconds when the load goes from over +2 KPa to less than -2 KPa. The surface loads range from reacting against the SMA to assisting the SMA actuation

and the temperature drops while the panel angle remains constant.

3.3 Five panel adaptive surface revised design.

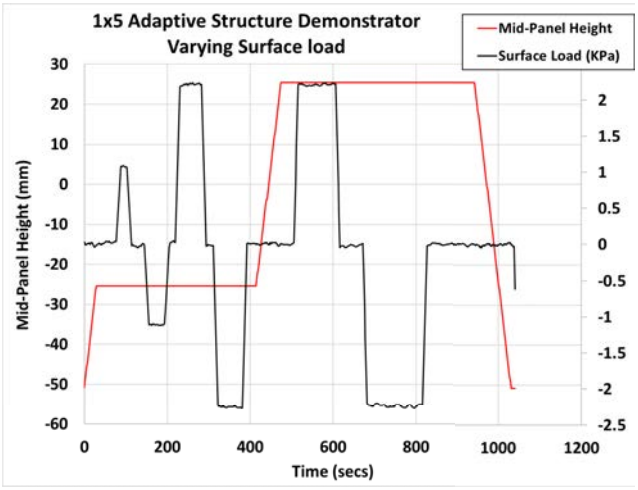

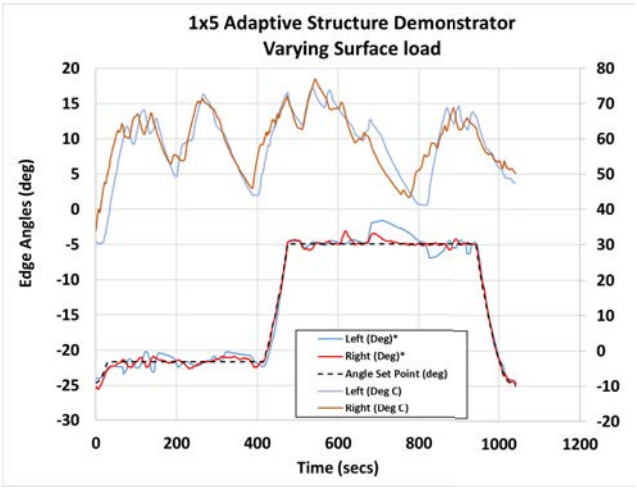

Figure 10: 1x5 panel constant shape with vary aerodynamic loads.

The rigid hinge design of the first five panel assembly limited the types of shapes that could be controlled and limited asymmetrical shapes as well as preventing a smooth surface when approaching a flat shape. A second 5 panel system was designed that added actuators to control hinge spacing on the middle panel, which allowed the total length to be controlled so that the panel was able to be go flat as it passed thought the center point. The width of the panels was varied to better create shapes that matched the geometries defined by the optimization team to mitigate sonic boom in adverse conditions. The electric linear servo on the center panel was replaced by an SMA based system similar to the rack and pinion design used in the first hardware demonstrator.

The revised design is shown in **Figure 11**. Profiles showing the surface as the system transitions from a dent to a bump is shown in **Figure 12**. The ability of the adaptive surface to flatten as it passes through the midpoint is clearly evident in (3). By controlling the spacing on the mid-panel hinge attachment points, the overall length of the surface is reduced,

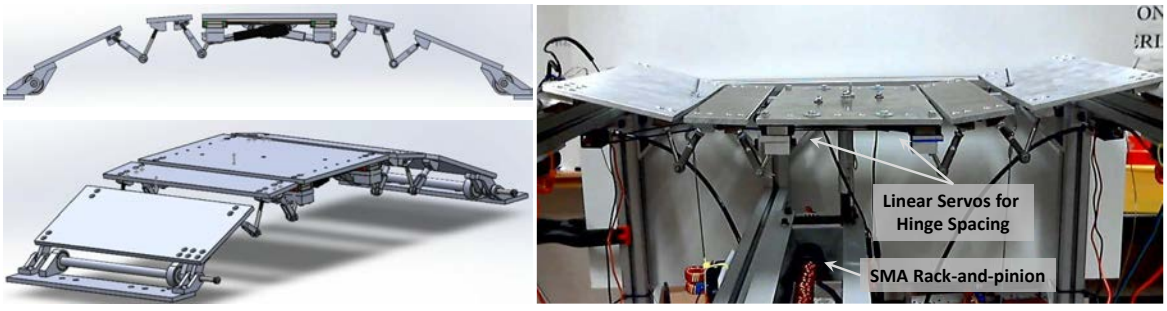

Figure 11: Revised 5 panel design.

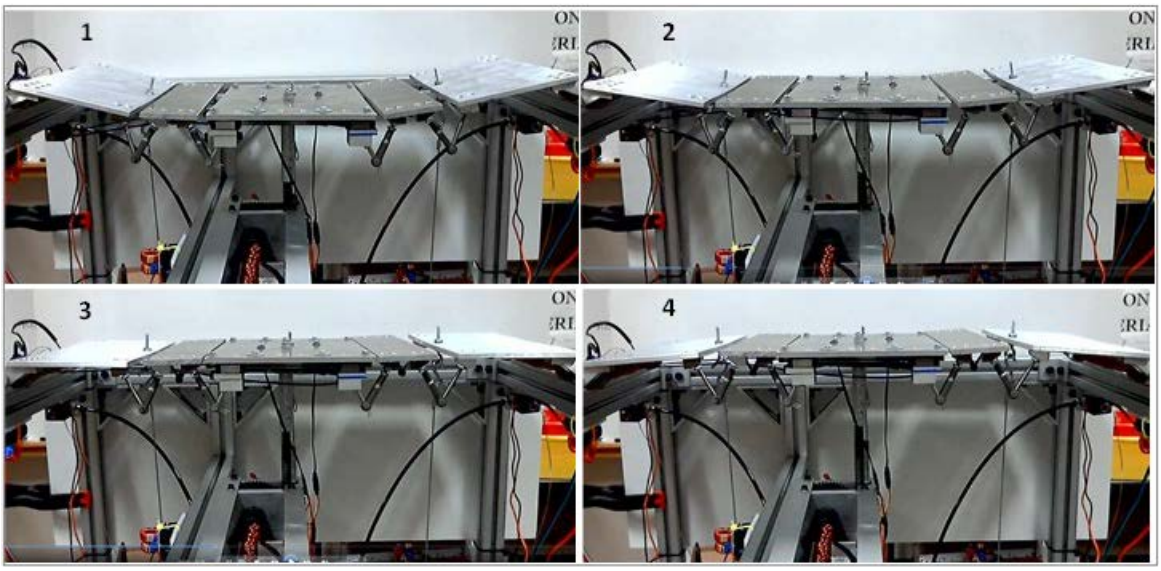

Figure 12: Revised 5 panel design transitioning through full range.

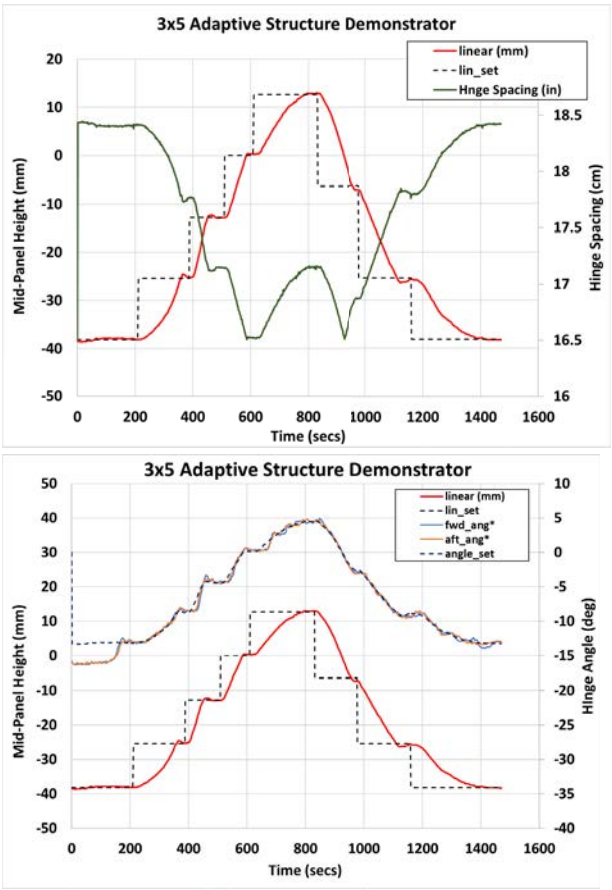

Figure 13: Revised 1x5 panel shape control

measured from outer hinge to outer hinge, enabling a flat profile.

Control of the mid-panel height and shape is shown in **Figure 13**. In the upper chart the mid-panel height and hinge spacing is shown as the surface transitions from a negative arc to a positive arc and back again. As the surface approaches the midpoint the hinge spacing is reduced, reaching minimum as the panel becomes flat, and then increasing as the panel expands outward into a arch.

In the lower chart the SMA edge panel angles are shown. For these tests the setpoint for the edge panels is a function of the mid-panel height. The upper dashed line shows the angle setpoint clearly tracking the mid-panel height and the SMA control system matching the setpoint

closely.

4 FLIGHT SIMULATOR INTEGRATION

The objective of the final hardware demonstration was to develop a connection between the as-built hardware geometries and the optimized OML deformations that were being modeled in the CFD based sonic boom minimization studies. This integrated system included the SMA based adaptive geometry hardware, supersonic flight simulation, atmospheric profiles based on publicly available NOAA data, simulated LIDAR measurements of the atmosphere below the aircraft, nearfield pressure signature prediction based on shapes generated by the hardware, and atmospheric propagation of pressure signatures. The system demonstration implemented a morphing map that correlated OML shapes to minimum boom shape predictions based on Mach, angle of attack, and atmosphere for a morphed X-59 aircraft.

For the demonstration, the single hardware morphing surface was extended and modeled as seven 1x5 panels spanning the fuselage of NASA's X-59 demonstrator. The distribution of the array of panels allowed for modeling deformations similar to the Gaussian bumps and dents that had been studied by the CFD and optimization teams. The development framework of the final demonstrator is shown in the flowchart of **Fig. 14**.

A major challenge for the technical demonstrator was producing realistic flight conditions for an overland supersonic flight. The opensource flight simulator FlightGear was selected for this work. The simulator provided a supersonic aircraft profile and autopilot for real-time flight simulation within the final demonstrator framework as well as positional data for a simulated overland supersonic flight. The longitude and latitude produced through this simulation was used to scrape weather data from the NOAA database using tools developed by the ULI project. This weather data included the temperature, humidity, and wind profiles necessary for pressure signature propagation using the NASA sBOOM code. The final

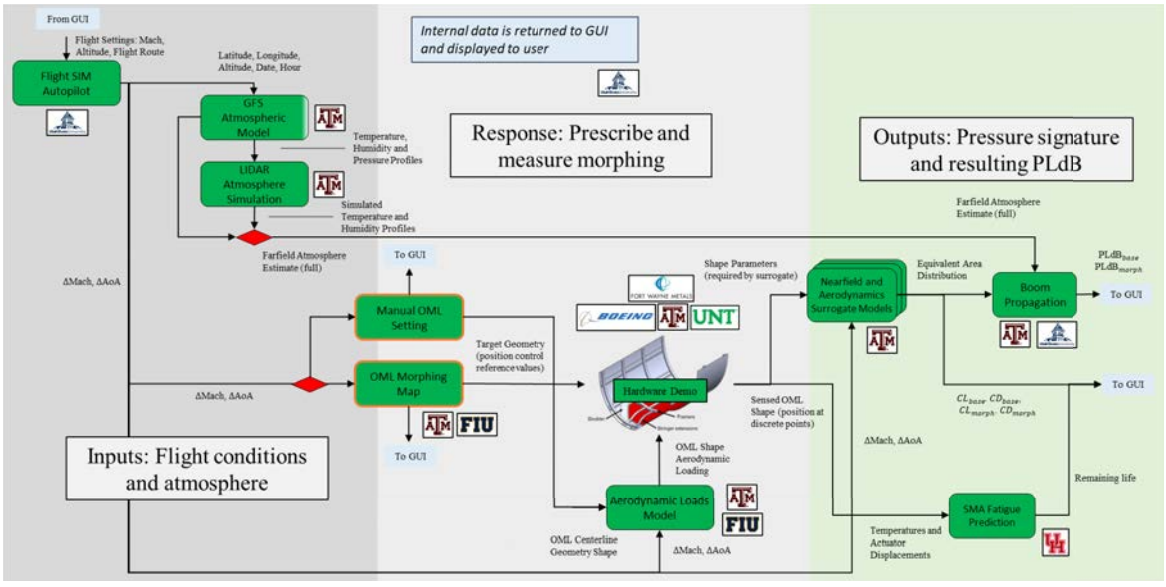

Figure 14: Developmental framework for integrated adaptive structure demonstration.

demonstrator framework also implemented simulated LIDAR temperature measurement noise using code developed by Texas A&M.

The hardware morphing map took flight data in the form of Mach number and angle-of-attack and produced an optimized set of morphing hardware parameters, representing the center panel displacement of the morphing regions on the X-59. These morphing parameters provided combinations of deformations that were found to reduce the PLdB of the X-59 under the specific flight condition.

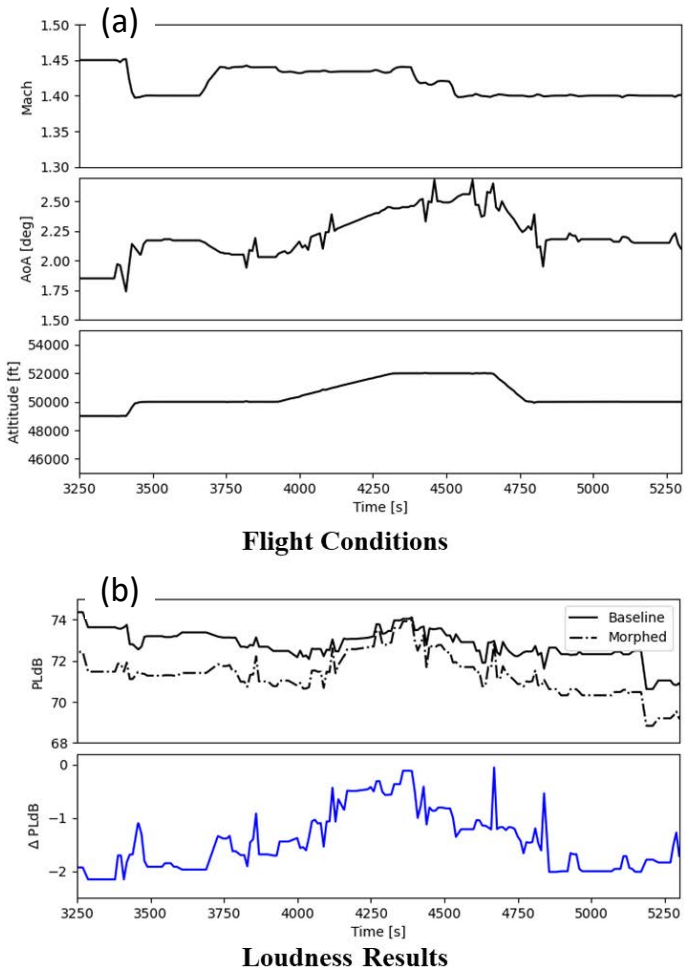

Figure 15: Cross country flight simulation of morphing OML for noise reduction.

The center panel displacements prescribed using the morphing map were passed to the physical hardware demonstrator. As the physical hardware was actuated to achieve the prescribed shape, real-time hardware measurements were reported to the integration framework code. The nearfield signature produced by the X-59 with the current hardware shape was then predicted using a nearfield surrogate model. The predicted nearfield signature was propagated using the NASA sBOOM code to produce a ground signature and ultimately the PLdB of the morphed X-59 aircraft under the current flight, hardware, and atmospheric conditions.

The framework of tools developed for the end-of-project demonstration was used to study and record data for a portion of an overland United States flight. They simulated a cross-country flight beginning in Seattle and passing through waypoints in Boise, Denver, and Dallas on the way to Miami. Occasional changes to Mach number and altitude were prescribed throughout the flight to instigate varying flight conditions for the morphing hardware to respond to. While the cross country simulation did not include the physical hardware in the demonstration loop, measured data was used to represent a response in hardware shape to changing flight conditions. **Fig. 15a** shows the

changes to Mach number, angle-of-attack, and altitude for a portion of the flight. **Fig. 15b** shows perceived noise on the ground and the reduction in perceived noise due to the OML morphing for the flight conditions of **Fig. 15a**. The most notable result is the constant reduction in perceived noise throughout the flight due to the shape changes prescribed by the morphing map.

5 CONCLUSIONS

Three SMA based adaptive structure hardware demonstrators were designed, built, and tested by a team of undergraduate students at Texas A&M, with the support of faculty, staff and industry advisors. The adaptive surfaces represented the center keel line of a supersonic vehicle and modified the OML shape to minimize the perceived sonic boom loudness under changing vehicle configurations and atmospheric profiles. The final demonstrator was integrated into a flight simulator which demonstrated real time shape modifications in response to changing flight conditions in order to minimized predicted noise for all flight conditions.

ACKNOWEDGMENTS

This work is supported by the NASA University Leadership Initiative (ULI) program under federal award number NNX17AJ96A, titled Adaptive Aerostructures for Revolutionary Civil Supersonic Transportation.

REFERENCES

[1] Carpenter, Forrest L., Paul G. Cizmas, Sohail R. Reddy, and George S. Dulikravich. “Controlling Sonic Boom Loudness Through Outer Mold Line Modification: A Sensitivity Study.” AIAA Scitech 2019 Forum (January 6, 2019). doi: https://doi.org/10.2514/6.2019-0603

[2] David S. Lazzara, Todd Magee, Hao Shen, James H. Mabe, Pedro B. Leal and Darren J. Hartl. "A Decoupled Method for Estimating Non-Ideal Sonic Boom Performance of Low-Boom Aircraft Due to Off-Design Flight Conditions and Non-Standard Atmospheres," AIAA 2021-1271. AIAA Scitech 2021 Forum. January 2021

[3] Lazzara, David S., Todd Magee, Hao Shen, and James H. Mabe. “Sonic Boom Performance of Low-Boom Aircraft in Non-Standard Atmospheres.” AIAA Scitech 2020 Forum (January 5, 2020).

[4] Weaver-Rosen, Jonathan M., Pedro BC Leal, Darren J Hartl, and Richard J Malak. “Parametric optimization for morphing structures design: application to morphing wings adapting to changing flight conditions.” Structural and Multidisciplinary Optimization. July, 2020. doi: https://doi.org/10.1007/s00158-020-02643-y

[5] Jonathan M. Weaver-Rosen, Forrest L. Carpenter, Paul G. Cizmas, Richard J. Malak, Troy A. Abraham, Douglas F. Hunsaker and David S. Lazzara, Computational Design Methodology of Adaptive Outer Mold Line for Robust Low En-Route Noise of a Supersonic Aircraft, AIAA Scitech 2021 Forum. AIAA 2021-0877. January 2021. doi: https://doi.org/10.2514/6.2021-0877

[6] Mabe, James H., Dimitris C. Lagoudas, and Darren Hartl. “Shape Memory Alloy Actuation Technology for Adaptive Low Boom Supersonic Transports.” 9th ECCOMAS Thematic Conference on Smart Structures and Materials, SMART 2019 (July 2019), pg. 462-472. imne.com/smart2019/frontal/doc/EbookSMART2019.pdf